International Journal of Thermophysics, Vol. 26, No. 1, January 2005 (© 2005)
DOI: 10.1007/s10765-005-2376-9

Application of the Inhomogeneous Sample Model in Piezoelectric Photothermal Spectroscopy of $Zn_{1-x}Be_xTe$ and $Cd_{1-x}Mn_xTe$ Mixed Crystals[1]

M. Malinski[2,3] and J. Zakrzewski[4]

This paper presents the basic details of the inhomogeneous sample model. This is one of the models that can be used for describing piezoelectric photothermal (PPT) spectra observed for mixed crystals. The experimental PPT spectra of $Zn_{1-x}Be_xTe$ and $Cd_{1-x}Mn_xTe$ mixed crystals presented in this paper exhibited the character of the crystal structure that was interpreted with the model of the inhomogeneous sample. The analysis of the spectra, performed with this model, enabled determination of both the basic optical parameters of the two crystal regions observed in the investigated samples and the composition of the crystals.

KEY WORDS: mixed crystals; photothermal piezoelectric detection; semiconductors.

1. INTRODUCTION

Piezoelectric photothermal (PPT) spectroscopy has recently become a practical method for the thermal and optical characterization of mixed semiconductor materials [1–4]. Recent advances in this field showed that this method enables determination of both optical and thermal parameters

[1]Paper presented at the Fifteenth Symposium on Thermophysical Properties, June 22–27, 2003, Boulder, Colorado, U.S.A.

[2]Department of Electronics, Technical University of Koszalin, 17 Partyzantow Street, 75-411 Koszalin, Poland.
[3]To whom correspondence should be addressed. E-mail: mmalin@tu.koszalin.pl
[4]Instytut Fizyki, Uniwersytet Mikolaja Kopernika, ul. Grudziadzka 5/7, 87-100 Torun, Poland.

of semiconductor samples. It revealed, however, the necessity of development of a series of physical models of real samples. The analysis showed that the conclusions drawn from experimental piezoelectric amplitude and phase spectra of the PPT signal depend in an essential way on the choice of the physical model of a sample. It turned out that one of the multilayer models of the sample, i.e., the inhomogeneous sample model, is one of the most important models for the case of mixed crystals. In this paper the inhomogeneous sample model is described in detail and the results of computations performed with this model are compared with the results of computations performed in a single-layer model. The results presented in this paper comprise the computations of the amplitude PPT spectra of $Zn_{1-x}Be_xTe$ and $Cd_{1-x}Mn_xTe$ mixed crystal samples at different frequencies of modulation in the range from 3 to 126 Hz. For simplicity the model in the two crystal regions approach is presented. All of the computed spectra are compared with experimental spectra obtained for the same set of frequencies. The most significant are the results obtained for $Zn_{1-x}Be_xTe$ mixed crystals in which the inhomogeneous character of the distribution of beryllium ions was clearly seen.

2. SAMPLE PREPARATION AND EXPERIMENTAL PROCEDURES

Single crystals of AII–BVI semiconductors analyzed in this paper were grown from a melt by the high-pressure Bridgman method under argon overpressure [5]. AII and BVI signify elements from the second and sixth columns of a periodic table, respectively. The crystals were cut into 0.1 cm thick plates, mechanically polished, and chemically etched. Some samples were annealed in zinc vapor at 1230 K for several hours. The PPT spectra were measured in the rear configuration with the piezoelectric transducer attached to the backside of the sample. For the measurements the open acoustic cell was used [6]. The signal was detected with a lock-in amplifier. All PPT spectra were measured at room temperature.

3. INHOMOGENEOUS SAMPLE MODEL

One can expect, in three-component mixed crystals, that the spatial distribution of ions in the crystal can be nonuniform. For example, in the case of $Zn_{1-x}Be_xTe$ mixed crystals, exhibiting an average value $x = 0.07$, a spatial distribution of Be is not uniform over the whole volume of the crystal. As a result, different parts of the crystal exhibit different optical parameters. There are several multilayer models describing different types of spatial distributions in the crystals: a single-layer model, an inactive layer model, the inhomogeneous sample model, a depletion layer

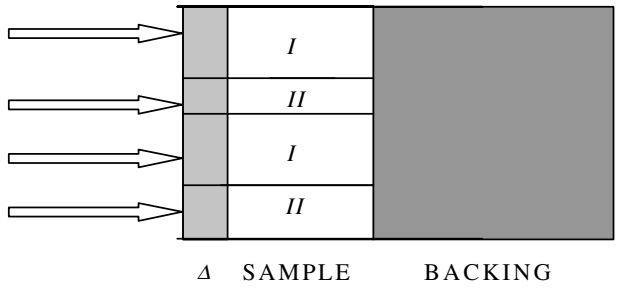

Fig. 1. Schematic diagram of a sample in the inhomogeneous sample model. I and II denote two crystal regions, Δ is the thickness of a surface inactive layer, and backing means in the case of investigated samples a steel hemisphere between the sample and a piezoelectric transducer.

model, an enriched layer model, or a model of superposition [7–9]. In this paper the inhomogeneous sample model is described in detail and illustrated with the experimental amplitude PPT spectra. In the model presented below, the PPT spectra were computed in the two crystal region approach, i.e., it is assumed that there are only two types of crystal regions exhibiting different optical parameters. A schematic diagram of a crystal sample in the inhomogeneous sample model is presented in Fig. 1. The inhomogeneity of a crystal was modelled with columns I and II exhibiting the same or similar thermal but different optical parameters. According to the model the crystal is of columnar type only to the thickness equal to the optical absorption length of the absorbed light in the crystal.

The spectra of the optical absorption coefficient of regions I and II are determined by a set of basic parameters. The expressions describing the optical absorption coefficient spectra in the low and high absorption regions of semiconductor samples exhibiting direct electron type transitions are given by the following expressions:

$$\text{For } E_{\text{exc}} < E_{\text{g}} \quad \beta(h\nu) = \beta_0 \exp\left((E_{\text{exc}} - E_{\text{g}})\gamma/(kT)\right) \tag{1}$$

$$\text{For } E_{\text{exc}} > E_{\text{g}} \quad \beta(h\nu) = A_0\sqrt{E_{\text{exc}} - E_{\text{g}}} + \beta_0 \tag{2}$$

E_{g} is the energy gap, E_{exc} is the energy of exciting photons, k is the Boltzmann constant, T is the temperature, A_0 is the optical absorption factor, and γ is the thermal or compositional broadening factor.

The set of average values of these parameters obtained for $Zn_{1-x}Be_xTe$ mixed crystals when $x = 0.07$ is given below.

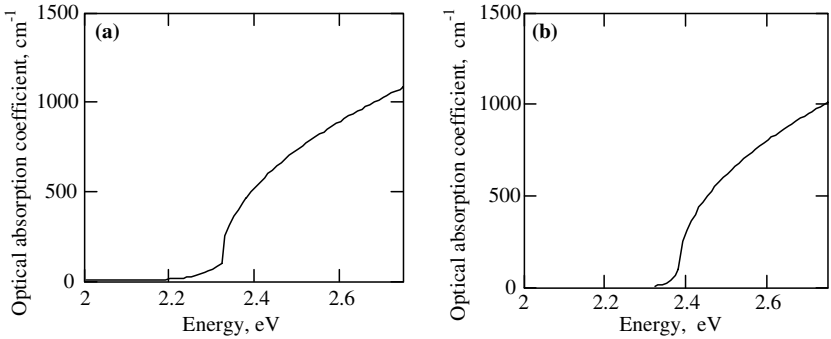

Fig. 2. Optical absorption coefficient spectra of the two crystal regions; (a) the first region exhibiting $E_{g1} = 2.32\,\text{eV}$ and (b) the second region of $E_{g2} = 2.38\,\text{eV}$.

$E_{g1} = 2.32\,\text{eV}$	$E_{g2} = 2.38\,\text{eV}$
$\beta_{01} = 100\,\text{cm}^{-1}$	$\beta_{02} = 80\,\text{cm}^{-1}$
$\gamma_1 = 0.5$	$\gamma_2 = 1$
$A_{01} = 1500\,\text{cm}^{-1} \cdot \text{eV}^{-1/2}$	$A_{01} = 1500\,\text{cm}^{-1} \cdot \text{eV}^{-1/2}$
$\alpha = 0.2\,\text{cm}^2 \cdot \text{s}^{-1}$	$\Delta = 0.006\,\text{cm}$

The values of the thermal diffusivities and thermal reflection coefficients R for the crystals analyzed in this paper were determined from separate frequency domain PPT phase characteristics [10,11]. The optical absorption coefficient spectra of these regions are presented in Fig. 2. It must be emphasized here that the spectra presented in Fig. 2 are the spectra computed from the fitting of the theoretical PPT spectra to experimental ones. The correctness of the spectra is limited to the value of about $500\,\text{cm}^{-1}$ because of the saturation region. Computer simulations indicated, however, that this fact does not influence the correctness of the procedures and considerations presented below. What changes is the thickness of an inactive layer that is extracted from the fitting procedure.

The PPT amplitude spectra computed for the above optical parameters and a thickness of the sample $l = 0.1\,\text{cm}$, a thermal diffusivity of the samples $\alpha = 0.2\,\text{cm}^2 \cdot \text{s}^{-1}$, a thermal reflection coefficient between the sample and the backing $R = -1$, a weighting parameter w describing the composition of an inhomogeneous crystal, and a frequency of modulation $f = 126\,\text{Hz}$ are presented in Fig. 3. The computations of the PPT spectra for each of the crystal regions separately were performed, both in a modified single-layer Jackson and Amer model [12] and in an inactive layer model, with new temperature spatial distribution formulae $T(x)$ derived in a thermal wave interference model [13,14] where $T(x)$ is, in fact,

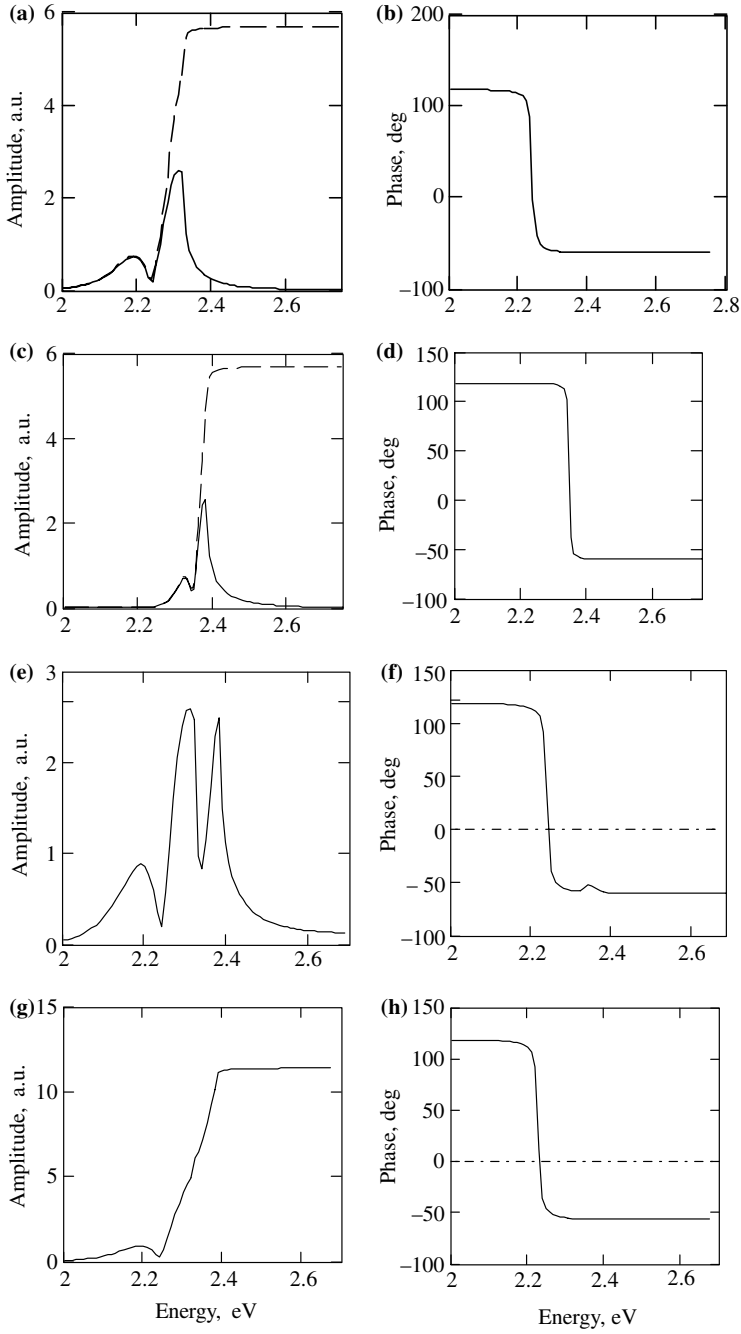
(a)
Amplitude, a.u.
(b)
Phase, deg
(c)
Amplitude, a.u.
(d)
Phase, deg
(e)
Amplitude, a.u.
(f)
Phase, deg
(g)
Amplitude, a.u.
Energy, eV
(h)
Phase, deg
Energy, eV

◀ **Fig. 3.** Amplitude and phase PPT spectra of the first (a, b) and the second (c, d) crystal regions. Dashed lines are the theoretical curves computed in a single-layer model, and solid lines are the theoretical curves computed in a model of an inactive layer with a thickness of an inactive layer $\Delta = 0.006$ cm; (e, f) amplitude and phase spectra of an inhomogeneous sample with the weighting parameter $w = 0.4$ and $\Delta = 0.006$ cm; and (g, h) amplitude and phase spectra of an inhomogeneous sample with $w = 0.4$ and $\Delta = 0$ cm where w is the weighting factor determining the composition of the crystal.

a function of many parameters $T(x, \alpha, f, l, \beta, R)$.

$$
\begin{aligned}
T(x) &= \frac{\beta I_0 \exp(-\beta\Delta)}{2\lambda\sigma(1-\exp(-2\sigma l))}[M(x)+N(x)] \\
M(x) &= \frac{[\exp(\sigma x)+\exp(-\sigma x)][\exp((-\sigma-\beta)x)-\exp((-\sigma-\beta)l)]}{\beta+\sigma} \\
&\quad + \frac{R\exp(-2\sigma l)[\exp(\sigma x)+\exp(-\sigma x)][\exp((\sigma-\beta)x)-\exp((\sigma-\beta)l)]}{\beta-\sigma} \\
N(x) &= \frac{[\exp(-\sigma x)+R\exp(-2\sigma l+\sigma x)][1-\exp((-\sigma-\beta)x)]}{\beta+\sigma} \\
&\quad + \frac{[\exp(-\sigma x)+R\exp(-2\sigma l+\sigma x)][1-\exp((\sigma-\beta)x)]}{\beta-\sigma}
\end{aligned} \tag{3}
$$

The computed piezoelectric signal is given by the Jackson and Amer equation,

$$
S \cong -C\left(\frac{1}{l}\int_0^l T(x)dx - \frac{6}{l^2}\int_0^l \left(\frac{l}{2}-x\right)T(x)dx\right) \tag{4}
$$

A general conclusion that can be drawn from an analysis of the diagrams of Fig. 3 is that the inhomogeneous character of the crystal can be easily recognized only for the case of samples with an inactive layer, Fig. 3e, f, because of the characteristic structure of the amplitude PPT spectrum. For the case of samples exhibiting a perfect quality surface, the recognition of the complex composition of the crystal is difficult (Fig. 3g, h).

Figure 3a, c above illustrate the influence of an inactive layer on the PPT amplitude and phase spectra. An inactive layer decreases strongly the value of the amplitude of the signal for energies above the energy gap of the crystal in the so-called high absorption region. It does not influence at the same time the phase spectra. An inactive layer can be considered as a thin surface layer of a semiconductor sample exhibiting a few times smaller thermal conductivity than the rest of a sample but with the same optical parameters. It results in a smaller value of the thermal diffusivity of this layer and a negative thermal reflection coefficient R between the layer and the substrate. Such surface layers, of amorphous type, were

observed, for example, in ion-implanted samples. They can be reduced by the annealing process that causes their recrystalization and enhancement of their thermal conductivity. The influence of such layers on the frequency characteristics of the PA signal was first analyzed and presented by Benett and Patty [15].

In a model of the inhomogeneous sample it is assumed that the measured piezoelectric signal is a superposition of two piezoelectric signals S_1 and S_2 coming from the two crystal regions with a weighting factor w. The resulting piezoelectric signal is given by the following equation:

$$S(h\nu) = S_1(h\nu)(1-w) + S_2(h\nu)w \tag{5}$$

The proposed model of an inhomogeneous sample depends on many thermal and optical parameters and a weighting parameter. This model of a sample was chosen after analysis of different models of samples and shapes of their PPT spectra computed with these models at different frequencies of modulation. The dependences of the shapes of amplitude and phase PPT spectra on the physical model of a sample were analyzed and described elsewhere [7–9]. Computations of the piezoelectric spectra presented in this paper were performed in a program FullDrum4R in Mathcad 2000 Professional. This program enables computations of the amplitude and phase PPT spectra in the inhomogeneous sample model for different optical, thermal, and experimental parameters and a given value of a weighting parameter. This program was also applied for the fitting procedures of theoretical curves to experimental spectra.

The experimental PPT spectra of $Zn_{1-x}Be_xTe$ mixed crystals were analyzed in the single-layer and inhomogeneous sample models. The amplitude PPT spectra of ZnTe crystals were examined as reference samples. They are presented in Fig. 4.

The PPT amplitude spectra exhibited an energy gap value of ZnTe crystals equal to $E_g = 2.28\,\text{eV}$. In the whole range of frequencies applied, i.e., from 3 to 126 Hz, the character of all spectra was similar to that presented in Fig. 4. Only differences in the values of the amplitude of the piezoelectric signal were observed. The $Zn_{1-x}Be_xTe$ mixed crystals exhibited, however, PPT spectra different from those observed for ZnTe crystals. Apart from the shift of the energy gap of the crystals from 2.28 eV for pure ZnTe crystals, to an average value of 2.35 eV for mixed crystals with a beryllium content $x = 0.07$, the spectra showed a considerable change of the shape with the frequency of modulation. This fact indicated the possibility of the existence of the complex crystal structure of the samples [16–19]. These experimental PPT spectra were then the focus of modeling with the inhomogeneous sample model. Figures 5–9,

presented below, show the experimental and theoretical amplitude PPT spectra of $Zn_{0.93}Be_{0.07}Te$ mixed crystals for different frequencies of modulations. Although the fits are not perfect, the theoretical curves reflect the character of the changes of the spectra with the frequency of modulation.

The change of the PPT spectra with the frequency of modulation is the result of the multiple reflections of the thermal waves originally generated in the sample, from the backing material. For the samples analyzed above exhibiting a thermal diffusivity $\alpha = 0.2\,\mathrm{cm}^2 \cdot \mathrm{s}^{-1}$, a thickness $l = 0.1\,\mathrm{cm}$, and low frequencies of modulation, they were thermally thin and this influence was strong. The influence of the reflections from the backing on the temperature distribution in the sample, and as a consequence on the spectrum of the piezoelectric signal, is stronger for the low absorption region than for the case of the high absorption one. That is why the low absorption part of the PPT spectra is modified stronger with the frequency of modulation than the high absorption one, and as a result, a deformation of the PPT spectra is observed. If this explanation is correct, then the change of the PPT spectra with the frequency of modulation should not be observed for the thermally thick samples where the contribution of the effect of reflection of thermal waves from the backing is negligible. This possibility of explanation of the observed changes was next examined for CdTe crystals.

The analysis of the PPT spectra of $Cd_{1-x}Mn_xTe$ crystals is presented below. As in the case of $Zn_{1-x}Be_xTe$ crystals, CdTe crystals exhibited only

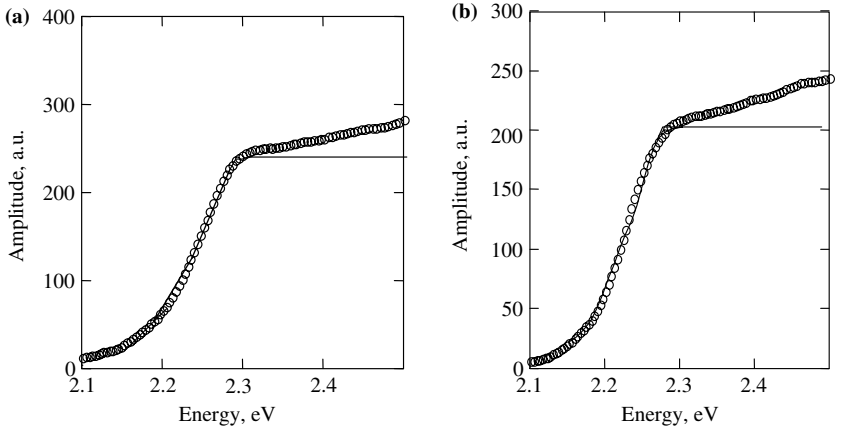

Fig. 4. PPT amplitude spectra of ZnTe at (a) $f = 16\,\mathrm{Hz}$ and (b) $f = 36\,\mathrm{Hz}$. Circles show experimental results, and solid lines are theoretical curves computed in a single-layer model with $\Delta = 0\,\mathrm{cm}$ and a quantum efficiency of band-to-band irradiative recombination $\eta = 1$.

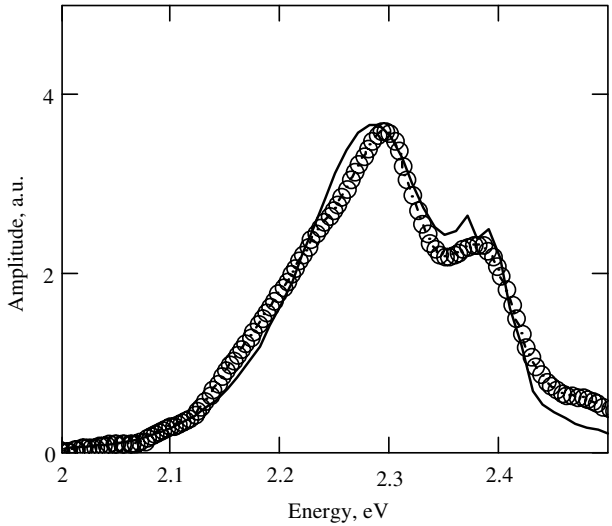

Fig. 5. Amplitude PPT spectra for $f = 3\,\text{Hz}$, $E_{g1} = 2.37\,\text{eV}$, $E_{g2} = 2.42\,\text{eV}$, and $w = 0.42$. Circles—experimental results and solid line—theoretical curve.

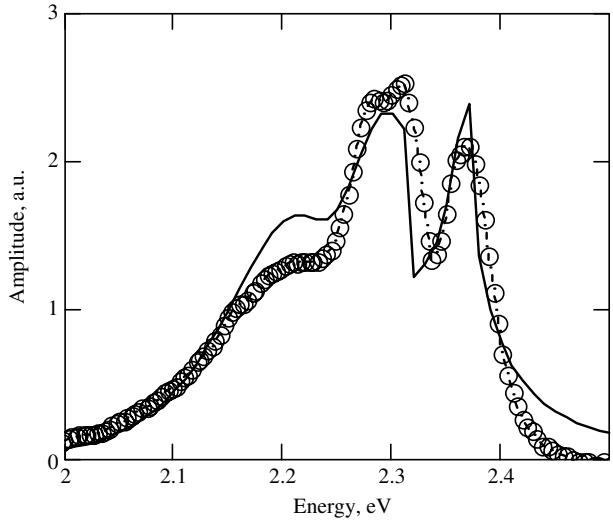

Fig. 6. Amplitude PPT spectra for $f = 16\,\text{Hz}$, $E_{g1} = 2.31\,\text{eV}$, $E_{g2} = 2.37\,\text{eV}$, and $w = 0.42$. Circles—experimental results and solid line—theoretical curve.

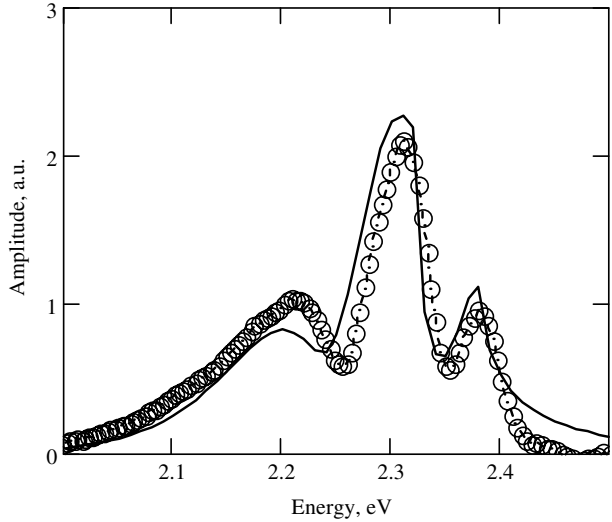

Fig. 7. Amplitude PPT spectra for $f = 36\,\text{Hz}$, $E_{g1} = 2.32\,\text{eV}$, $E_{g2} = 2.38\,\text{eV}$, and $w = 0.25$. Circles—experimental results and solid line—theoretical curve.

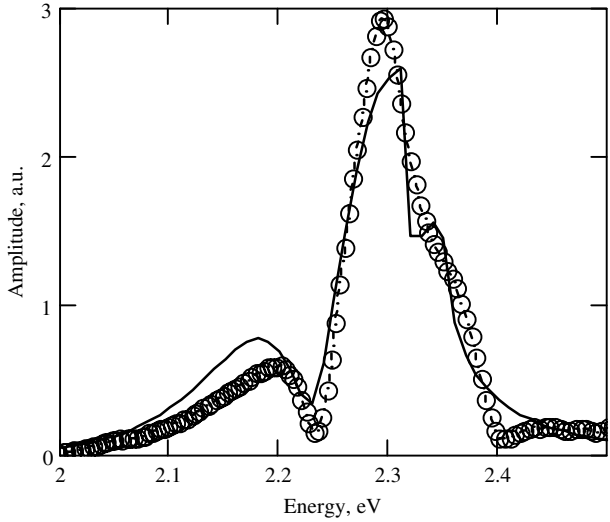

Fig. 8. Amplitude PPT spectra for $f = 76\,\text{Hz}$, $E_{g1} = 2.31\,\text{eV}$, $E_{g2} = 2.35\,\text{eV}$, and $w = 0.25$. Circles—experimental results and solid line—theoretical curve.

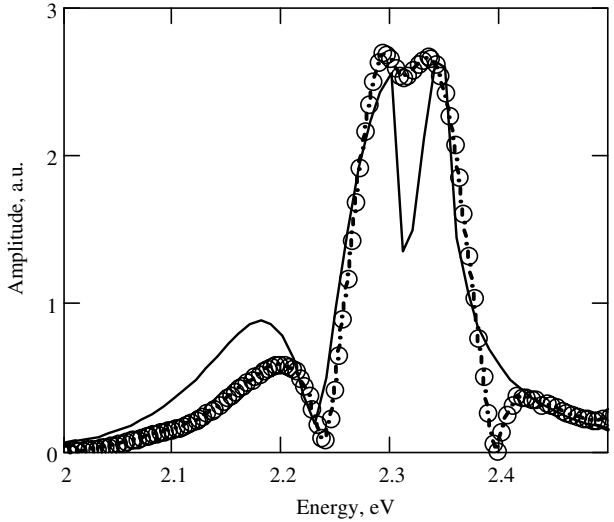

Fig. 9. Amplitude PPT spectra for $f = 126\,\text{Hz}$, $E_{g1} = 2.30\,\text{eV}$, $E_{g2} = 2.35\,\text{eV}$, and $w = 0.4$. Circles—experimental results and solid line—theoretical curve.

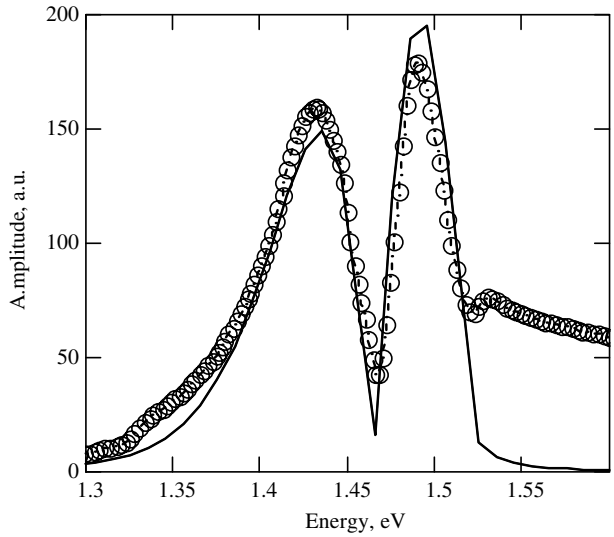

Fig. 10. Amplitude PPT spectra of CdTe sample at $f = 76\,\text{Hz}$. Circles—experimental results, and a solid line is the theoretical curve computed for the parameters: $E_g = 1.51\,\text{eV}$, $\alpha = 0.03\,\text{cm}^2 \cdot \text{s}^{-1}$, $\Delta = 0.019\,\text{cm}$, $\beta_0 = 130\,\text{cm}^{-1}$, and $\gamma = 0.9$.

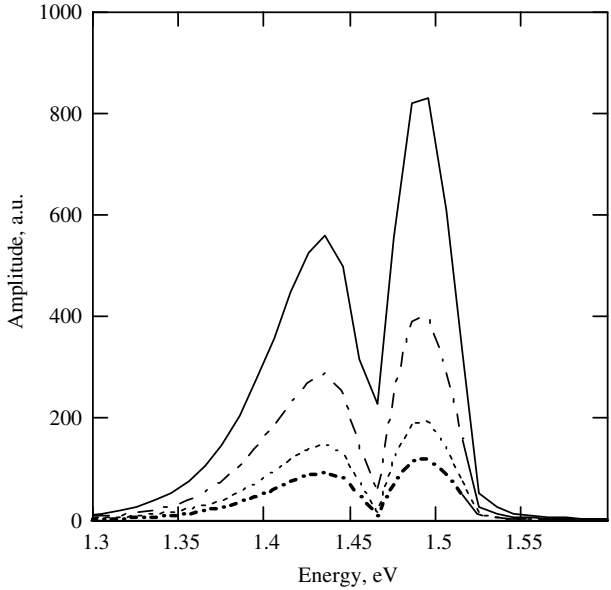

Fig. 11. Amplitude characteristics of a CdTe crystal at different frequencies of modulation: $f = 16\,\text{Hz}$—solid line, $f = 36\,\text{Hz}$—dashed-dotted line, $f = 76\,\text{Hz}$—dotted line, and $f = 126\,\text{Hz}$—dashed line with $\alpha = 0.03\,\text{cm}^2 \cdot \text{s}^{-1}$, and $R = -0.6$.

one crystal region with an energy gap $E_g = 1.51\,\text{eV}$ while crystals with the addition of Mn ions, i.e., $Cd_{1-x}Mn_xTe$ crystals, exhibited a complex crystal structure composed of two crystal regions exhibiting an average energy gap value $E_g = 2.05\,\text{eV}$. Their PPT spectra were analyzed in the inhomogeneous sample model. The influence of the frequency of modulation on the change of the shape of the spectra is also shown and discussed. The amplitude PPT spectra of a CdTe sample are presented in Fig. 10.

CdTe crystals exhibit a low thermal diffusivity $\alpha = 0.03\,\text{cm}^2 \cdot \text{s}^{-1}$, and the thermal diffusion length is relatively short which makes the samples thermally thick in the range of frequencies 16–126 Hz. In this case the influence of the backing is small. The theoretical amplitude PPT spectra of a CdTe sample at different frequencies of modulation are presented in Fig. 11.

For the case of the thermal and experimental parameters applied for CdTe crystals, the shape of the amplitude PPT spectra does not depend on the frequency of modulation. Only the total value of the piezoelectric signal decreases with an increase of the frequency of modulation. The study of the influence of an order of magnitude increase of the thermal

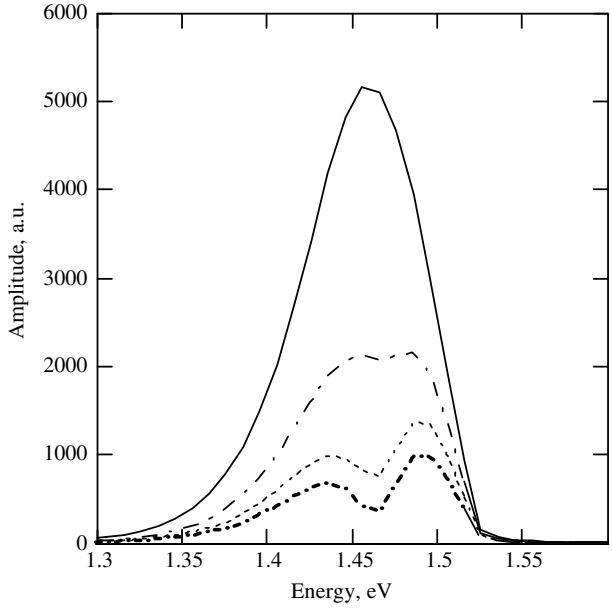

Fig. 12. Amplitude characteristics of CdTe crystals at different frequencies of modulation: $f = 16\,\text{Hz}$—solid line, $f = 36\,\text{Hz}$—dashed-dotted line, $f = 76\,\text{Hz}$—dotted line, and $f = 126\,\text{Hz}$—dashed line but computed for $\alpha = 0.3\,\text{cm}^2 \cdot \text{s}^{-1}$, i.e., 10 times larger than for the case of Fig. 10; $R = -0.6$.

diffusivity on the PPT amplitude spectra is shown in Fig. 12. Because the thermal diffusion length is now over three times longer, a change of the shape of the spectra with a decrease of the frequency of modulation was expected. In this case, it turned out that the shape of the spectra changed considerably with frequency. The results of computer analysis agree with the results of measurements performed for $Cd_{1-x}Mn_xTe$ mixed crystals [20]. The PPT spectrum of the $Cd_{0.51}Mn_{0.49}Te$ mixed crystal is presented in Fig. 13. This spectrum exhibited two crystal regions with two different energy gaps $E_{g1} = 2.035\,\text{eV}$ and $E_{g2} = 2.105\,\text{eV}$, corresponding to different concentrations of Mn ions, $x = 0.42$ and 0.47, respectively, and two different thicknesses of the inactive layer, $\Delta_1 = 0.005\,\text{cm}$ and $\Delta_2 = 0\,\text{cm}$. Investigations of a series of $Cd_{1-x}Mn_xTe$ samples showed that different samples can exhibit different thicknesses of an inactive layer depending on the concentration of Mn ions. The physical explanation of this fact is not known at present. $Cd_{1-x}Mn_xTe$ crystals are more thermally insulating than $Zn_{1-x}Be_xTe$ crystals as they show a thermal diffusivity in the range $\alpha = 0.005$–$0.1\,\text{cm}^2 \cdot \text{s}^{-1}$. Measurements of the PPT spectra

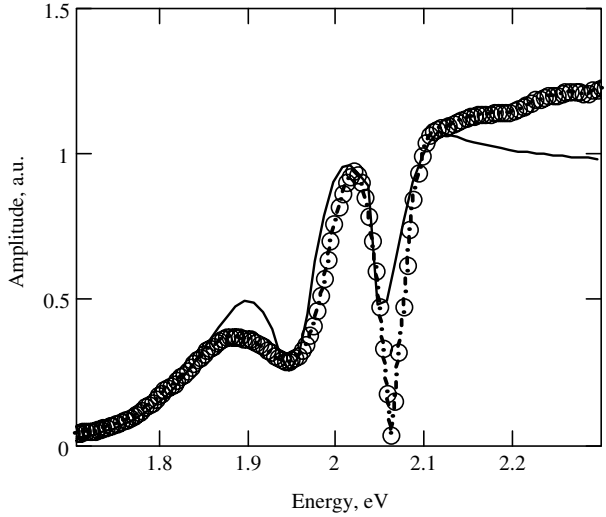

Fig. 13. Amplitude PPT spectra of $Cd_{0.51}Mn_{0.49}Te$ mixed crystals for $f = 76\,Hz$, $l = 0.1\,cm$. Fitting parameters: $E_{g1} = 2.035\,eV$, $\beta_{01} = 130\,cm^{-1}$, $\gamma_1 = 0.5$, $A_{01} = 1500\,cm^{-1} \cdot eV^{-1/2}$, $E_{g2} = 2.105\,eV$, $\beta_{02} = 150\,cm^{-1}$, $\gamma_2 = 0.9$, $A_{02} = 1500\,cm^{-1} \cdot eV^{-1/2}$, $\alpha = 0.1\,cm^2 \cdot s^{-1}$, $\Delta_1 = 0.005\,cm$, $\Delta_2 = 0\,cm$, $R = 1$, and $w = 0.3$. Circles—experimental results and solid line—theoretical curve.

of $Cd_{0.51}Mn_{0.49}Te$ mixed crystals, for frequencies of modulation $f = 6$, 36, and 126 Hz, showed that all the spectra were identical with the one presented in Fig. 13 measured at $f = 76\,Hz$.

The computations performed with the inhomogeneous sample model also gave the same shape of the spectra for all these frequencies of modulation. No visible change of the shape of the PPT spectra was observed with a change of the frequency of modulation. This fact confirms the proposed explanation of the observed changes of the PPT amplitude spectra of thermally thin $Zn_{1-x}Be_xTe$ mixed crystals.

The experimental photoacoustic amplitude and phase frequency characteristics obtained with a microphone detection, measured later on the same $Zn_{1-x}Be_xTe$ mixed crystal samples in the transmission configuration, confirmed the correctness of the inhomogeneous sample model and the crystal structure of investigated mixed crystals. The conclusions presented in this paper were also confirmed by the numerical analysis of the PPT phase spectra of the same crystals performed in the inhomogeneous sample model and presented in Ref. 21.

4. CONCLUSIONS

The general conclusion that was drawn from the results of computations performed with the inhomogeneous sample model was the following. It enables the determination of the composition of the crystals described by the weighting parameter "w." It is possible to control the uniformity of the spatial distribution of components in the crystal. This model enables also a quantitative description of the quality of the surface with the parameter Δ, which is the thickness of an inactive layer. By fitting the theoretical amplitude PPT spectra to the experimental ones, it is possible to determine a set of basic optical parameters of the crystal regions. A physical reason for the observed changes of the PPT spectra, with the frequency of modulation, was proposed. It is based on the model of reflections of thermal waves, generated in the sample, from the backing material.

REFERENCES

1. F. Firszt, S. Legowski, H. Meczynska, J. Szatkowski, and J. Zakrzewski, *AIP Conf. Proc.* **463**:530 (1999).
2. J. Zakrzewski, F. Firszt, S. Legowski, H. Meczynska, and M. Pawlak, *Proc. Deutsche Gesellschaft für Akustik* (DEGA e.V., Forschritte der Akustik DAGA 02, Bochum 2002, Germany), p. 436 (CD).
3. H. Meczynska, J. Zakrzewski, S. Legowski, M. Popielarski, F. Firszt, J.Szatkowski, R.Klugiewicz, and K. Legowski, *Acta Phys. Polon. A* **87**:547 (1995).
4. J. Zakrzewski, F. Firszt, S. Legowski, H. Meczynska, M. Pawlak, and A. Marasek, *Rev. Sci. Instrum.* **74**:566 (2003).
5. F. Firszt, H. Meczynska, B. Sekulska, J. Szatkowski, W. Paszkowicz, and J. Kachniarz, *Semicond. Sci. Technol.* **10**:197 (1995).
6. H. D. Breuer, *Proc. 1st Int. Conf. on Photoacoustic Effect in Germany* (1981), p. 115.
7. M. Malinski, J. Zakrzewski, and H. Meczynska, *Proc. Deutsche Gesellschaft für Akustik* (DEGA e.V., Forschritte der Akustik DAGA 02, Bochum 2002, Germany), p. 430 (CD).
8. M. Malinski, Mol. Quantum Acoustics **23**:277 (2002).
9. M. Malinski and J. Zakrzewski, *Rev. Sci. Instrum.* **74**:598 (2003).
10. M. Malinski, J. Zakrzewski, and H. Meczynska, *Proc. 4th Int. Conf. Thermal and Mechanical Simulation EuroSIME 2003* (2003), p. 199.
11. M. Malinski, *Phys. Stat. Sol. (a)* **198**:169 (2003).
12. W. Jackson and N. M. Amer, *Appl. Phys.* **51**:3343 (1980).
13. M. Malinski, *Arch. Acoust.* **27**:217 (2002).
14. M. Malinski, *Arch. Acoust.* **28**:43 (2003).
15. C. A. Benett and R. R. Patty, *Appl. Optica* **21**:49 (1982).
16. J. Zakrzewski, Ph. D. Thesis (Univ. Mikolaja Kopernika, Torun, 2001).
17. J. Zakrzewski, F. Firszt, S. Legowski, H. Meczynska, and A. Marasek, *Proc. Deutsche Gesellschaft für Akustik* (DEGA e.V., Forschritte der Akustik DAGA02, Bochum 2002, Germany), p. 438 (CD).
18. W. Paszkowicz, F. Firszt, S. Legowski, H. Meczynska, J. Zakrzewski, and M. Marczak, *Phys. Stat. Sol. (b)* **229**:57 (2002).

19. F. Firszt, S. Legowski, H. Meczynska, J. Szatkowski, and J. Zakrzewski, *Anal. Sci.* **17**:129 (2001).
20. J. Zakrzewski, F. Firszt, S. Legowski, H. Meczynska, A. Marasek, and M. Pawlak, *Rev. Sci. Instrum.* **74**:572 (2003).
21. M. Maliński, *Photoacoustics and Photoacoustic Spectroscopy of Semiconductor Materials* (Technical University of Koszalin, Koszalin, 2004).